Histol Histopathol (2024) 39: 117-130

Histology and Histopathology
From Cell Biology to Tissue Engineering

ORIGINAL ARTICLE Open Access

KRT80 expression works as a biomarker and a target for differentiation in gastric cancer

Kai-hang Shi[1], Hang Xue[1], En-hong Zhao[2], Li-jun Xiao[3], Hong-zhi Sun[4] and Hua-chuan Zheng[1]

[1]Department of Oncology and Central Laboratory, [2]Department of Surgery (3), The Affiliated Hospital of Chengde Medical University, [3]Department of Immunology, Basic Medicine College of Chengde Medical University, Chengde and [4]Cancer Center, The First Affiliated Hospital of Jinzhou Medical University, Jinzhou, China

Summary. Keratin 80 (KRT80) is a filament protein that participates in cell differentiation and the integrity of the epithelial barrier. Here, KRT80 expression was higher in gastric cancer compared with normal mucosa at both mRNA and protein levels by bioinformatic analysis, qRT-PCR and Western blot ($p<0.05$), however, the methylation of KRT80 was lower than in normal mucosa ($p<0.05$). There was a negative relationship between promoter methylation and expression level of KRT80 gene in gastric cancer ($p<0.05$). KRT80 mRNA and protein expression was positively correlated with the differentiation of gastric cancer ($p<0.05$), while KRT80 methylation was negatively associated with gastric cancer differentiation and p53 mutation ($p<0.05$). The expression of KRT80 mRNA was positively linked to the short survival time of gastric cancers ($p<0.05$). The differential genes of KRT80 mRNA were involved in ligand-receptor interaction, estrogen signal pathway, peptidase, filament and cytoskeleton, keratinocyte differentiation, vitamin D receptor, muscle contraction, and B cell-mediated immunity ($p<0.05$). KRT80-related genes were classified into cell adhesion and junction, cadherin binding, skin and epidermis development, and so forth ($p<0.05$). KRT80 knockdown suppressed proliferation, anti-apoptosis, anti-pyroptosis, migration, invasion and epithelial-mesenchymal transition in gastric cancer cells ($p<0.05$). These findings indicated that up-regulated expression of KRT80 played a crucial part in gastric carcinogenesis, and might be considered as a biological marker for aggressive behaviors and poor prognosis. Its silencing might be used as an approach of target therapy for gastric cancer patients.

Corresponding Author: Professor Huachuan Zheng, Department of Oncology and Central Laboratory, The Affiliated Hospital of Chengde Medical University, Chengde 067000, China. e-mail: zheng_huachuan@hotmail.com

www.hh.um.es. DOI: 10.14670/HH-18-618

Key words: Gastric cancer, KRT80, Biological behaviors, Prognosis, Gene therapy

Introduction

Gastric cancer (GC) is a global health problem, and nearly half of all new cases and deaths happen in China each year (Fan et al., 2021). Moreover, the prevalence is higher in less developed countries than in highly developed countries worldwide (Thrift and Nguyen, 2021). The majority of GCs are discovered at an advanced stage with a negative prognosis. The accuracy, reliability, and safety of gastroendoscopy screening have been constrained by its invasive screening methodology and the need for professional endoscopists and pathologists. Increasing age, male sex, non-White race, Helicobacter pylori infection, dietary habit, and smoking were all found as risk factors for GC (Yang et al., 2020). Despite advancements in GC patient management and treatment, the overall result remains poor. Recently, both phage display selection and tailoring subtractive cells have been widely used to discover novel antibodies, which hold the potential for biomarkers and therapeutic interventions (Khajeh et al., 2018; Mehdipour et al., 2020).

As an adaptive response to altered gravity, extracellular matrix proteins, adhesion molecules, and cytoskeletal proteins form a dynamic network that interacts with signaling molecules. Keratins are intermediate filament (IF) cytoskeletal proteins that maintain the structural integrity of epithelial cells, and are considered as representative markers for epithelial cells, and molecular diagnostic biomarkers for oral squamous cell carcinoma, basal cell carcinoma, hepatocellular carcinoma, stomach adenocarcinoma, bladder cancer, breast cancer and cervical cancer (Langbein et al., 2010; Lin et al., 2020). Keratins can be classified into two types: 28 acidic or type I (KRT9KRT40) and 26 basic or neural type II (KRT1-KRT8, KRT71-KRT86). Keratin 80 (KRT80, K80),

along with Keratins 7, 8, and 78, is a type II keratin (Langbein et al., 2010; Li et al., 2018; Lin et al., 2020). The KRT80 gene, which is found on chromosome 12q13, encodes a 452-amino-acid protein with an estimated molecular mass of 50.5 kDa and an isoelectric point of 5.47. Another smaller alterative variant included just 422 amino acids and had an isoelectric point of 5.08 and a calculated molecular mass of 47.2 kDa. KRT80 is a filament protein that makes up one of the major structural fibers of epithelial cells (Langbein et al., 2010; Li et al., 2018; Lin et al., 2020). This was also illustrated in the non-α-helical KRT80 end domains, which contained a multitude of proline and cysteine residues, as well as the complete absence of GGX or GGG repeats, which are generally located in the head and tail domains of most type II epithelial keratins (Langbein et al., 2010; Li et al., 2018; Lin et al., 2020).

Langbein et al. (2010) found that KRT80 strongly resembled type II hair keratins more than type II epithelial keratins structurally. KRT80 expression is related to advanced tissue or cell differentiation. The KRT80-containing IFs are found close to the desmosomal plaques at the cell margins, in which they are tightly crosslinked with the cytoplasmic IF bundles. In contrast, KRT80 adopts the "traditional" cytoplasmic distribution in cells undergoing terminal differentiation. KRT80 is one of the earliest keratins, with evidence dating back to fish. Additionally, alternative splicing affects KRT80 mRNA. Aside from KRT80, we describe KRT80.1, a smaller but completely functioning splice variation that evolved solely in mammals. Unlike KRT80, which is generally expressed, KRT80.1 is only found in soft and hard keratinizing epithelial tissues of the hair follicle and the filiform tongue papilla. Rajagopalan et al. (2016) demonstrated that skin moisture was linked to increased expression of KRT80, as well as caspase 14 and filaggrin. Castellucci et al. (2021) revealed that KRT80 was lower in cutaneous leishmaniasis (CL) caused by Leishmania braziliensis than the control according to GWAS.

Reportedly, miR-4268 suppressed gastric carcinogenesis through inhibiting KRT80 (Zhang et al., 2022). KRT80 promoted migration, invasion and EMT of non-small cell lung cancer cells by the TGF-β/Smad pathway (Tong et al., 2022). Liu et al. (2021) found that KRT80 regulated by miR-206/ETS1 aggravated proliferation, migration and invasion and EMT of ovarian cancer cells via the MEK/ERK pathway. Ouyang et al. (2022) found that OTUB2 silencing inhibited the proliferation of GC cells although the proliferative capacity was restored upon KRT80 re-supplementation. OTUB2 stabilized KRT80 by deubiquitinating and suppressing proteasome-mediated degradation through Lys-48 and Lys-63. Zhang et al. (2022) demonstrated that KRT80 mRNA expression was closely associated with lymph node metastasis, nodal status, CEA, CA199, pathological differentiation, TNM stage and defective mismatch repair of GC using qRT-PCR, and poor prognosis using bioinformatics analysis. In the present study, we aimed to investigate the clinicopathological and prognostic significances of KRT80 expression in combination of bioinformatics, qRT-PCR, Western blot and immunohistochemistry, and clarify the relevant molecular mechanisms in GC.

Materials and methods

Cell culture and transfection

Gastric cancer (SGC-7901) cells were obtained from the Chinese Academy of Sciences' Cell Bank in Shanghai, China. They were incubated at 37°C in a humidified environment of 5% CO_2 and RPMI 1640 medium supplemented with 10% fetal bovine serum (FBS), 100 units/mL penicillin, and 100g/mL streptomycin. KRT80 siRNA (sc-96163, Santa cruz) was bought for the gene silencing with control siRNA (sc-37007, Santa cruz) as negative control.

In a 6-well plate, 2×10^5 cells per well was cultured in 2 ml antibiotic-free RPMI-1640 supplemented with FBS until 60-80% confluence. The siRNA duplex solution (Solution A, sc-36868) was gently mixed and incubated with Transfection Reagent (Solution B, sc-36868) for 15-45 minutes at room temperature. After washing with 2 ml of siRNA Transfection Medium(sc-36868), the cells were incubated with the siRNA Transfection Reagent mixture (Solution A & B) at 37°C in an incubator for 5-7h. After that, we added 1 ml of normal growth medium containing 2× normal growth medium in the transfection well, and incubated the cells for the next 24h. Finally, we replaced the medium with fresh 1× normal growth medium and incubated the cells for 24h for the following experiments.

Proliferation assay

The Cell Counting Kit-8 was used to count the number of viable cells. 2.0×10^3 cells per well were planted on a 96-well plate and cultured until adherence. At multiple consecutive points in time, 10 μL of CCK-8 solution was added to each well of the plate, and the plates were incubated for 2h until being measured at 450 nm.

Apoptosis assay by flow cytometry

Flow cytometry was performed with Fluorescein isothiocyanate isomer (FITC)-labeled Annexin V (BD Pharmingen, USA) and Propidium Iodide (PI). Among them, FITC-labeled Annexin V was detected for phosphatidylserine externalization as an endpoint indicator of early apoptosis recommended by the protocol. And PI was used to detect late apoptosis and necrosis.

Wound healing assay

In 6-well culture plates, cells were seeded at a

density of 1.0×10^6 cells/well. After reaching confluence, the cell monolayer was scraped with a pipette tip to form a scratch, washed three times with PBS, and cultured in FBS-free medium. The cells were pictured at 0h, 24h and 48h of incubation and the scratch area was calculated using ImageJ software.

Cell migration and invasion experiments

In the migration assay, 2.5×10^5 cells were resuspended in serum-free RPMI 1640, and planted in the upper portion of the uncoated chamber (BD Bioscience). The lower part of the chamber contained 10% FBS as a chemoattractant. After 24h in the incubator, the cells were wiped on the membrane, cleaned with PBS, fixed in 100% methanol, and stained with crystalline violet. In the invasive assay, the insert membranes were coated with diluted matrigel (BD Bioscience), and the other procedures were consistent with the above.

Patients

The paraffin-embedded blocks of gastric non-neoplastic mucosa (n=224), primary cancer (n=261) and metastatic cancer in lymph node (n=32) were gathered during surgical excision in the First Affiliated Hospital of Jinzhou Medical University in China. Pathological specimens (including adjacent normal tissues) were obtained from the First Affiliated Hospital of Jinzhou Medical University and stored in a -80°C refrigerator from 2020 to 2021. Those samples were used for protein and RNA extraction, respectively. There had been no chemotherapy, radiation, or adjuvant treatment given to the patients prior to surgery. All patients signed informed consent forms prior to the start of the clinical trial. The Affiliated Hospital of Chengde Medical University's ethics committee gave us permission to perform clinical study.

Tissue microarray (TMA)

Pathological specimens were fixed in 4% paraformaldehyde, dehydrated with ethanol, dealcoholized with xylene and embedded in paraffin. For histological analysis, paraffin blocks were cut into 4 μm slices and stained with hematoxylin and eosin. Representative areas of adjacent normal tissues and solid tumors were identified by a microscope, and corresponding tissue cores were punched out of paraffin blocks and transferred to pathological blocks, which were incised into 4μm-thick.

qRT-PCR

As suggested by Bustin et al. (2009), total RNA of fresh specimens was isolated by the RNeasy mini kit (QIAGEN, Germany, 74104). The absorbance value (A) of RNA was determined using Nanodrop (Thermal), and the ratio of A260/A280 for RNA samples was determined to be within 1.8-2.0 for purity assessment. The quality was evaluated using denatured agarose gel electrophoresis. cDNA was reversely transcribed by M-MLV reverse transcriptase kit (Promega, M1701) and random primers (Takara). According to sequences from GenBank, Real-time primers were designed by primer-BLAST in NCBI. GAPDH primers were forward: 5′-GTCTCCTCTGACTTCAACAGCG-3′ and reverse: 5'-ACCACCCTGTTGCTGTAGCCAA-3′(131bp). KRT80 primers were forward: 5'-GCTGGTCGGCTGGCAC TATCT-3' and reverse: 5'-GCCTTCATCTCCTCCTTC TCCTG-3' (121bp). The iTaqTM universal SYBR® green supermix (BIO-RAD) was used to amplify cDNA by CFX96TM real-time system (BIO-RAD) with GAPDH as an internal control. Twenty microliter reaction mixtures contained 10 μl qPCR mix (×2) with 1.8 μl (10 μM) of each primer, and 80 ng of template cDNA. The protocol was an initial incubation at 95°C for 10 min, followed by 60 cycles of denaturation at 95°C for 30s, annealing at 55°C for 1min, and extension at 72°C or 30s.

Western blotting

RIPA lysis buffer was used to extract total proteins from cells and fresh samples, which were then quantified using the BCA kit. Proteins of equivalent volume were separated by 10% SDS-PAGE and transferred to PVDF membranes. Nonspecific antigen sites were blocked by five percent skim milk for 1.5h, and then incubated with rabbit anti-KRT80 (1:2000, Proteintech, 16835-1-AP), mouse anti-Bcl-2 (1:500, Santa Cruz, sc-7382), mouse anti-Bax (1:500, Santa Cruz, sc-7480), rabbit anti-Caspase-1 (1:2000, abcam, ab207802), rabbit anti-E-cadherin (1:5000, abcam, ab76319), mouse anti-N-cadherin (1:2000, abcam, ab280375), rabbit anti-Zeb1 (1:1000, ABclonal, A21794), mouse anti-Ki-67 (1:1000, Proteintech, 39799), rabbit anti-p-Stat3 (1:1000, Wanleibio, WLP2412), rabbit anti-p-Akt (1:1000, CST, 5012), rabbit anti-p21 (1:200, Santa Cruz, sc-397), rabbit anti-P38 (1:1000, CST, 14451), rabbit anti-Beclin-1 (1:500, Santa Cruz, sc-11427), rabbit anti-MMP-9 (1:1500, Proteintech, 10375-2-AP) mouse anti-PARP-1 (1:500, Santa Cruz, sc-8007), rabbit anti-Slug (1:5000, Abcam, ab302780), or mouse anti-GAPDH (1:2000, Hangzhou Goodhere, AB-M-M001) overnight at 4°C. After three washes, the membranes were treated with anti-rabbit or anti-mouse antibody with horseradish peroxidase (1:5000, CST, USA, #7074S) for 2h. Protein bands were obtained with C300 (Azure Biosystems) by the Western Bright™ ECL western blotting detection kit (Advansta, USA, K-12045-D50), and analyzed by Image J software (v1.8.0).

Immunohistochemistry (IHC)

The slides were deparaffinized and rehydrated 3 times respectively, and antigen retrieval was completed

in a microwave oven for 20 minutes. Endogenous peroxidase activity and non-specific binding sites were blocked for 30 minutes with 3% hydrogen peroxide (H_2O_2) and 5% bovine serum albumin (BSA), respectively. Then, the slides were incubated with rabbit anti-KRT80 (Proteintech, 1:80) for 3 hours at room temperature. After three PBS rinses, the slides were incubated at room temperature for two hours with polyclonal swine anti-rabbit antibody with HRP (1:200, DAKO, Japan, P0399). The specific binding sites were seen using diaminobenzidine (DAB). The slides were dehydrated, cleaned, mounted, and stained with hematoxylin for observation under a microscope (Nikon, Nikon Corporation, Japan).

Immunoreactivity to KRT80 was localized in the membrane and cytoplasm. Two independent researchers (SKH and ZHC) randomly selected 100 cells and counted them from five representative fields for the study. The positive rate classifications were as follows: 0=0%; 1=1-49%; 2=50-74%; 3≥75%. The positive intensity classifications were as follows: 1=weak; 2=medium; 3=strong. The immunohistochemical score was calculated as the intensity × positive rate, with the scores defined as follows: -=0; +=1-2; ++=3-5; +++=6-9.

Bioinformatics analysis

The expression and methylation of *KRT80* gene was analyzed with the Oncomine database (www.oncomine.org), xiantao platform (https://www.xiantao.love/), Timer database (https://cistrome.shinyapps.io/timer/) and/or UALCAN database (http://ualcan. path. uab.edu). To investigate the clinicopathological significance of KRT80, we used R software to extract transcript expression data (RNA-seqV2) and clinicopathological data of gastric cancer from the TCGA database. The prognostic significance of *KRT80* was explored by Kaplan-Meier plotter (http://kmplot.com/). Additionally, we found the differential and related genes using xiantao platform. The differential genes were subjected to the construction of the PPI network and selected out the important hub genes. These genes were submitted to KEGG and GSEA analysis in order to build signal pathways.

Statistical analysis

Spearman correlation analysis was employed to compare the rank counting data, and student t test to differentiate the means of two groups. Kaplan-Meier

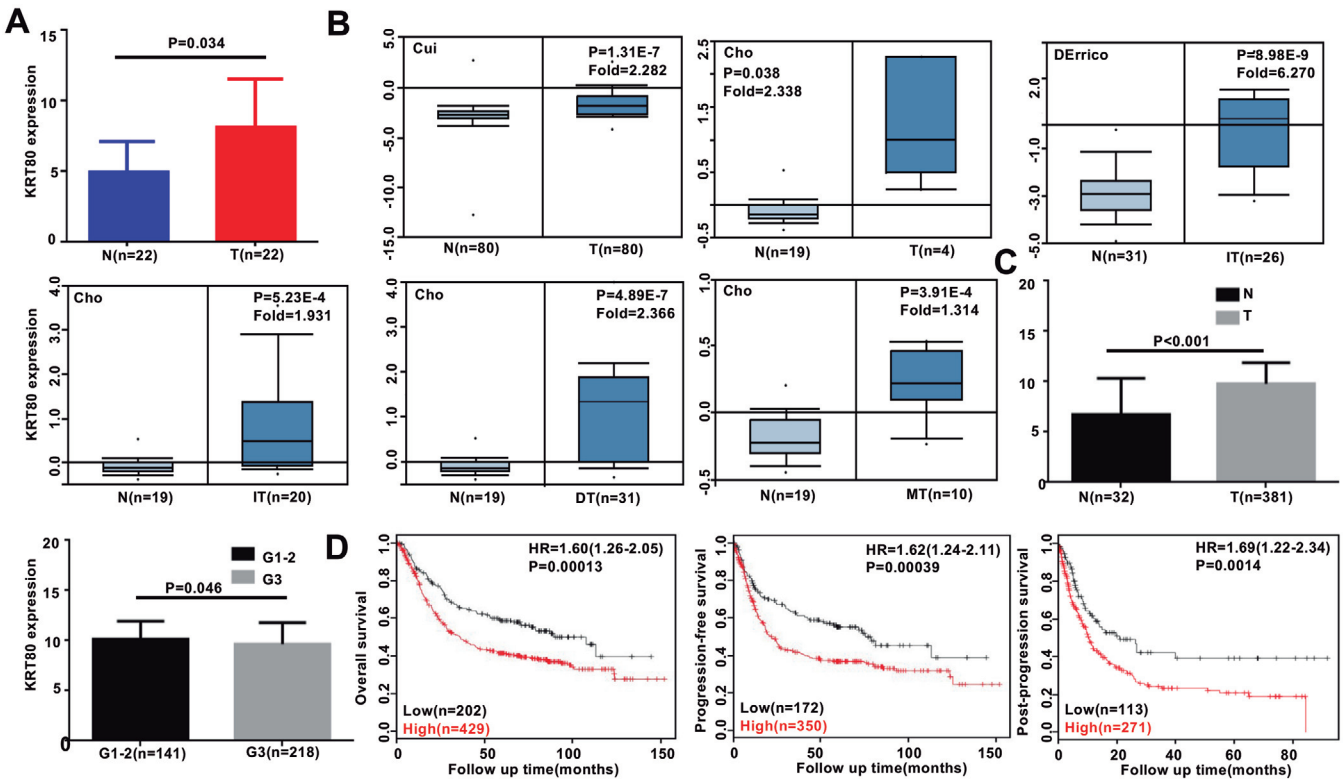

Fig. 1. The clinicopathological significance of KRT80 mRNA expression in gastric cancer. KRT80 mRNA expression was higher in gastric cancer than normal mucosa by quantitative RT-PCR **(A)**, Oncomine **(B)** and TCGA **(C)** databases ($p<0.05$). It was negatively correlated with histological grading (**B**, $p<0.05$) according to TCGA dataset, and overall, progression-free and post-progression survival of gastric cancer patients according to Kaplan-Meier plotters (**D**, $p<0.05$). N, normal mucosa; T, cancer; IT, intestinal-type adenocarcinoma; DT, diffuse-type adenocarcinoma; MT, mixed-type adenocarcinoma; G, histological grade; HR, hazard ratio.

plots and log-rank statistic were used to compare between the survival curves. We employed Cox's proportional hazards regression model to carry out survival multivariate analysis. All the data were analyzed using SPSS 24.0, then a two-tailed $p<0.05$ was regarded as statistically significant.

Results

KRT80 expression in gastric cancer: clinicopathological and prognostic implications

Quantitative RT-PCR revealed that KRT80 mRNA expression was higher in gastric cancer than in normal mucosa (Fig. 1A, $p<0.05$). Then, using Oncomine's Cui's, Cho's, and DErrico's datasets, we performed bioinformatics analysis and discovered that KRT80 mRNA was more expressed in gastric cancer than normal mucosa independent of Lauren's categorization subtypes (Fig. 1B, $p<0.05$). It was consistent with the KRT80 mRNA level according to the TCGA database (Fig. 1C, $p<0.05$). According to the TCGA dataset, it was adversely linked with histological grading of GC (Fig. 1C, $p<0.05$). As summarized in Table 1, KRT80 mRNA expression was not related to any clinicopathological aspects of GC using xiantao platform. ($p>0.05$).

As shown in Fig. 1D, a lower KRT80 mRNA expression was positively linked to overall survival, progression-free survival and post-progression survival of the GC patients by Kaplan-Meier plotter ($p<0.05$). As summarized in Table 2, Kaplan-Meier plotter showed

Table 1. The relationship between KRT80 expression and gastric cancer clinicopathological characteristics by xiantao database.

Characteristics	Group	Low expression	High expression	p
Age, n (%)	≤65	92 (24.8%)	72 (19.4%)	0.052
	>65	94 (25.3%)	113 (30.5%)	
Gender, n (%)	Female	68 (18.1%)	66 (17.6%)	0.884
	Male	119 (31.7%)	122 (32.5%)	
T stage, n (%)	T1	10 (2.7%)	9 (2.5%)	0.805
	T2	38 (10.4%)	42 (11.4%)	
	T3	82 (22.3%)	86 (23.4%)	
	T4	54 (14.7%)	46 (12.5%)	
N stage, n (%)	N0	59 (16.5%)	52 (14.6%)	0.769
	N1	48 (13.4%)	49 (13.7%)	
	N2	34 (9.5%)	41 (11.5%)	
	N3	36 (10.1%)	38 (10.6%)	
M stage, n (%)	M0	165 (46.5%)	165 (46.5%)	1.000
	M1	13 (3.7%)	12 (3.4%)	
Pathologic stage, n (%)	I	25 (7.1%)	28 (8%)	0.591
	II	61 (17.3%)	50 (14.2%)	
	III	72 (20.5%)	78 (22.2%)	
	IV	17 (4.8%)	21 (6%)	
Histologic grade, n (%)	G1	4 (1.1%)	6 (1.6%)	0.067
	G2	58 (15.8%)	79 (21.6%)	
	G3	119 (32.5%)	100 (27.3%)	

Table 2. The prognostic significance of KRT80 mRNA in gastric cancer by Kaplan-Meier plotter.

Clinicopathological features		Overall survival		Post-progression survival		Progression-free survival
		Hazard ratio	p	Hazard ratio	p	Hazard ratio
Sex	Female	1.88 (1.19-2.97)	0.0061	1.83 (1.11-3.02)	0.017	1.69 (1.11-2.57)
	Male	1.63 (1.12-2.37)	0.0099	1.73 (1.14-2.63)	0.0097	1.51 (1.11-2.04)
T	2	1.88 (1.19-2.98)	0.0062	1.72 (1.05-2.82)	0.029	1.82 (1.20-2.75)
	3	1.82 (1.28-2.58)	0.00067	2.13 (1.39-3.26)	4.0e-04	1.50 (1.07-2.10)
N	0	1.75 (0.75-4.11)	0.19	0.15 (0.02-1.13)	0.033	1.81 (0.77-4.23)
	1-3	1.75 (1.27-2.42)	0.00053	1.67 (1.19-2.35)	0.0029	1.61 (1.19-2.18)
	1	1.78 (1.05-3.02)	0.029	1.55 (0.92-2.60)	0.098	1.88 (1.13-3.12)
	2	2.97 (1.77-4.93)	1.5e-05	2.66 (1.55-4.57)	0.00024	2.45 (1.54-3.91)
	3	0.72 (0.42-1.23)	0.22	0.72 (0.41-1.28)	0.27	0.76 (0.44-1.32)
M	0	1.69 (1.24-2.32)	0.00094	1.65 (1.19-2.28)	0.0024	1.60 (1.19-2.16)
	1	1.95 (0.98-3.88)	0.053	2.86 (1.23-6.64)	0.011	1.39 (0.77-2.52)
TNM staging	1	1.71 (0.52-5.58)	0.37	2.72 (0.56-13.16)	0.20	1.82 (0.56-5.94)
	2	1.26 (0.68-2.35)	0.46	0.73 (0.636-1.49)	0.39	1.42 (0.78-2.58)
	3	2.48 (1.62-3.80)	1.6e-05	2.52 (1.59-4.01)	5.2e-05	2.24 (1.48-3.38)
	4	0.86 (0.58-1.28)	0.46	0.76 (0.49-1.19)	0.23	1.16 (0.75-1.79)
Perforation	-	2.00 (1.31-3.05)	0.0011	1.43 (0.81-2.54)	0.22	2.02 (1.35-3.03)
Treatment	Surgery alone	1.48 (1.09-2.02)	0.012	1.45 (1.04-2.03)	0.029	1.45 (1.09-1.92)
	5-FU-based adjuvant	5.13 (1.77-14.89)	0.00093	2.42 (0.86-6.80)	0.084	3.98 (1.53-10.32)
Differentiation	Moderately	3.71 (1.66-8.27)	0.00067	2.46 (0.88-6.88)	0.078	4.11 (1.85-9.10)
	Poorly	1.96 (1.19-3.22)	0.0073	1.67 (0.86-3.23)	0.13	1.86 (1.17-2.96)
Lauren's classification	Intestinal-type	2.77 (1.64-4.70)	7.85e-05	3.08 (1.67-5.67)	0.00014	2.55 (1.55-4.20)
	Diffuse-type	1.66 (1.15-2.41)	0.0069	1.68 (1.10-2.58)	0.016	1.74 (1.23-2.48)
Her2 positivity	-	1.55 (1.17-2.05)	0.0019	1.64 (1.13-2.37)	0.0079	1.55 (1.15-2.10)
	+	1.53 (1.02-2.29)	0.038	2.13 (1.18-3.87)	0.011	1.89 (1.18-3.02)

that a lower KRT80 mRNA expression was positively linked to overall, post-progression or progression-free survival rate of GC patients, regardless of sex, T staging, Lauren's classification, and Her-2 expression ($p<0.05$). This is also true for overall, post-progression or progression-free survival rate in the cancer patients with stage N1-3, stage N2, stage 3 and surgical-only gastric disease ($p<0.05$). KRT80 mRNA expression was positively associated with the overall or progression-free survival time of the cancer patients with N1, M0, poorly- or moderately-differentiated adenocarcinoma, no perforation, and 5-FU-based adjuvant ($p<0.05$). The same results of the post-progression survival were seen in the N0 cancer victims ($p<0.05$).

In addition, we discovered an inverse correlation between mRNA expression and promoter methylation (cg03747456, cg24174145, cg20225745, cg00280812, cg04472592 and cg16432350 sites) of KRT80 gene in GC by xiantao database (Fig. 2A, $p<0.05$). Also, KRT80 methylation was lower in stomach cancer than in normal mucosa (Fig. 2B, $p<0.05$) and was positively related to histological grading and p53 non-mutation status in GC (Fig. 2B, $p<0.05$) in terms of the UALCAN database.

As shown in Table 3, KRT80 mRNA expression was adversely related to the infiltration of B cell, CD8+ T cells, Cytotoxic cells, dendtric cells (DC), pDC, T cells,

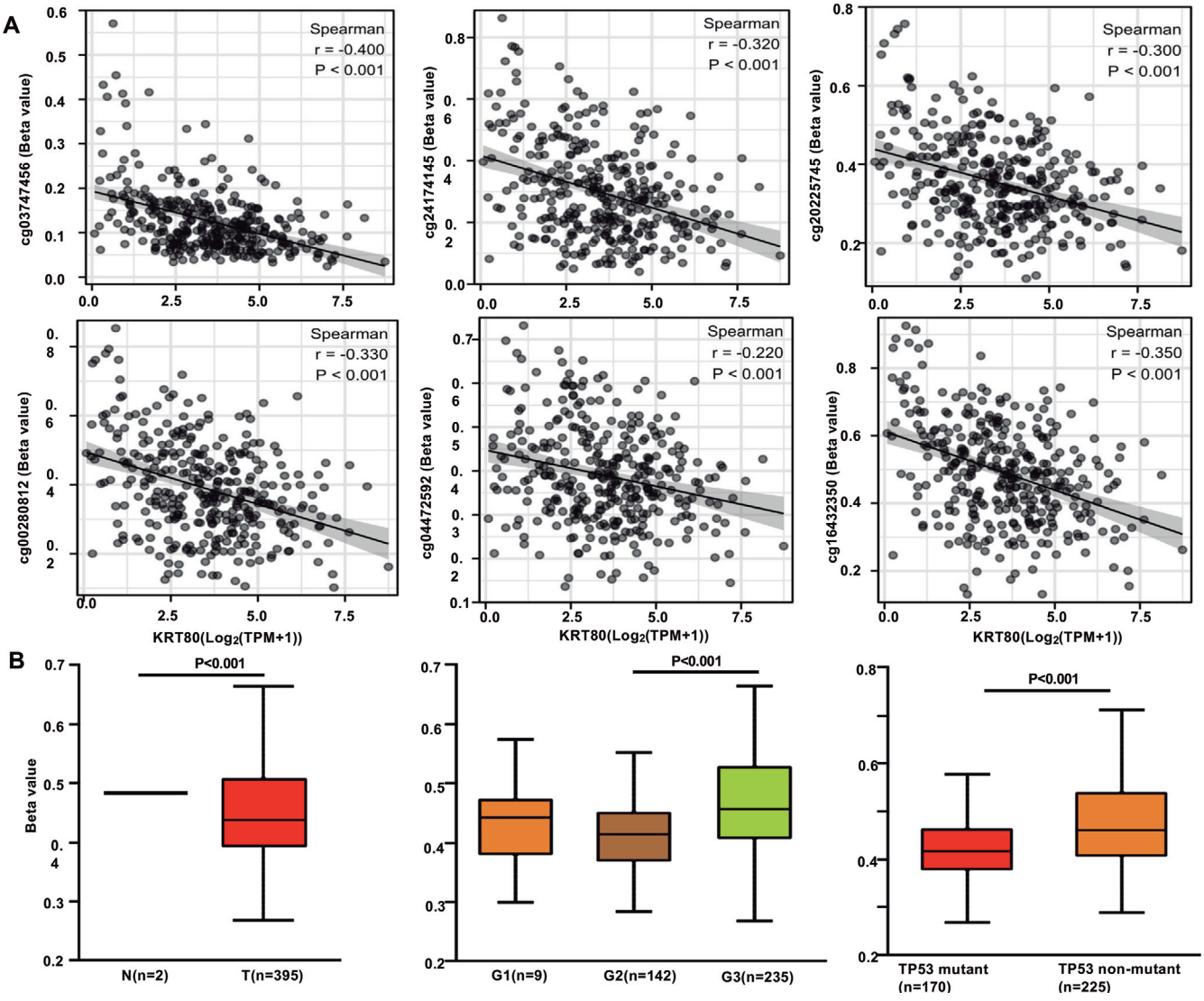

Fig. 2. The clinicopathological significance of KRT80 promoter methylation in gastric cancer. According to xiantao database, we found a negative relationship between mRNA expression and promoter methylation of KRT80 gene in gastric cancer (**A**, $p<0.05$). Additionally, KRT80 methylation was lower in gastric cancer than normal mucosa **(B)**, and was positively associated with histological grading and p53 non-mutation status of gastric cancer (**B**, $p<0.05$) in terms of UALCAN database. N, normal; T, tumor; G, histological grade; *, $p<0.05$.

T helper cells, Tem, TReg, TFH, and Tgd according to xiantao database ($p<0.05$). The outcomes of multivariate Cox's analysis confirmed that old age, cliniopathological staging 3-4, and infiltration of macrophages were independent risk factors for worse prognosis of GC patients in terms of the Timer database (Table 4, $p<0.05$).

The KRT-80-related genes and pathways in gastric cancer

On the xiantao platform, we found the differential genes between low and high expression groups of KRT80 mRNA in GC and built up the volcano map as Fig. 3A. KEGG analysis showed that the top signal pathways included ligand-receptor interaction, estrogen signal pathway, peptidase, filament and cytoskeleton, keratinocyte differentiation, and so on (Fig. 3B, $p<0.05$). GSEA analysis showed that the top signal pathways were composed of keratinization, NABA matrisome, vitamin D receptor, muscle contraction, CD22-mediated BCR regulation, B cell receptor signal, and so forth (Fig. 3C, $p<0.05$). In addition, the STRING was used to identify the PPI pairs (Fig. 4A) and the cytoscape to find out the top 10 nodes ranked by degree (Fig. 4B). According to xiantao database, SPRR3, SPRR1B, and SPRR2D were more expressed in gastric cancer than in normal tissues. (Fig. 4C, $p<0.05$).

Table 3. The relationship between immune infiltration and KRT80 mRNA expression by xiantao database.

Cell	Spearman	p
aDC	-0.090	0.081
B cells	-0.305	<0.001
CD8 T cells	-0.228	<0.001
Cytotoxic cells	-0.215	<0.001
DC	-0.156	0.003
Eosinophils	-0.035	0.503
iDC	-0.051	0.326
Macrophages	-0.070	0.179
Mast cells	-0.066	0.203
Neutrophils	0.004	0.937
NK CD56bright cells	0.103	0.046
NK CD56dim cells	-0.036	0.491
NK cells	0.065	0.210
pDC	-0.222	<0.001
T cells	-0.294	<0.001
T helper cells	-0.194	<0.001
Tcm	-0.092	0.074
Tem	-0.164	0.001
TFH	-0.244	<0.001
Tgd	-0.106	0.040
Th1 cells	-0.056	0.277
Th17 cells	-0.115	0.026
Th2 cells	-0.061	0.237
TReg	-0.117	0.023

DC, dendritic cell; Treg, regulatory T cell; Tcm, central memory T cells; Tem, effector memory T cell; TFH, follicular helper T cell; NK, natural killer. Tdg, γδ T cells.

According to the xiantao database, the positively-correlated genes of KRT80 in GC are shown in the heat map of Fig. 5A ($p<0.05$), and are involved in cell adhesion and junction, cadherin binding, skin and epidermis development, and so forth (Fig. 5B). The negatively-correlated genes of KRT80 in gastric cancer are shown in the heat map of Fig. 5C ($p<0.05$), and are involved in chemokine and cytokine signal pathway, immune response, antigen binding, primary immunodeficiency, T cell receptor and immunoglobulin complex, and so forth. (Fig. 5D). The KRT80-correlated genes (SLC2A1, KLK6, PMEPA1, SPTBN2, ADGRG1, TGFA, PERP and ADGRF4) were more expressed in gastric cancer than normal tissue (Fig. 5E, $p<0.05$), but the converse was true for PRKCB, BTG2 and PNOC (Fig. 5E, $p<0.05$).

The clinicopathological significance of KRT80 protein expression in gastric cancer

Immunohistochemically, KRT80 expression was positive in gastric superficial, fundus and body glands, and proper glands (Fig. 6A). Statistically, KRT80 expression was significantly higher in gastric cancer than non-tumorigenic mucosa (Table 5, $p<0.05$), but no

Table 4. The multivariate survival analysis of gastric cancer patients by Timer database.

Parameters	Co-efficiency	HR	95%CI	p
Age	0.036	1.037	1.015-1.059	0.001
Gender-male	0.230	1.259	0.811-1.955	0.306
Race-Black	0.492	1.635	0.653-4.095	0.294
Race-White	0.189	1.208	0.718-2.034	0.476
Stage 2	0.775	2.171	0.943-5.001	0.069
Stage 3	1.112	3.040	1.402-6.594	0.005
Stage 4	1.478	4.385	1.523-12.624	0.006
Purity	-0.512	0.599	0.267-1.345	0.215
B cells	4.815	123.305	0.988-15389.922	0.051
CD8+ T cells	-0.643	0.526	0.022-12.680	0.692
CD4+ T cells	-4.200	0.015	0.000-3.968	0.140
Macrophage	7.793	2423.816	54.132-108529.770	<0.001
Neutrophil	-2.549	0.078	0.000-163.786	0.514
Dendritic cells	0.701	2.017	0.100-40.606	0.647
KRT80 mRNA expression	0.053	1.054	0.920-1.208	0.446

HR, hazard ratio; CI, confidence interval.

Table 5. KRT80 expression in gastric carcinogenesis by immunohistochemistry.

Groups	n	KRT80 expression			
		-	+	++	+++
Non-neoplastic mucosa	224	132	58	32	2
Primary cancer	261	70	91	76	24
Metastatic cancer in lymph node	32	5	5	14	8

PR, positive rate; *, $p<0.001$.

difference was seen between primary and metastatic cancer (Table 5, $p>0.05$). As illustrated in Table 6, KRT80 expression was higher in intestinal-type than diffuse-type adenocarcinoma ($p<0.05$), but not related to the other clinicopathological characteristics of stomach cancer ($p>0.05$). Based on the densitometric analysis of Western blots, KRT80 expression was stronger in gastric cancer samples than in paired normal mucosa samples (Fig. 6B, $p<0.05$). The expression of KRT80 in gastric epithelial cells and oncocytes was screened by Western blot, and SGC-7901 cells were selected for the following cell function experiments (Fig. 6C).

The impact of KRT80 expression on the phenotypes of stomach cancer cells

Following siRNA transfection, KRT80 protein expression was reduced in SGC-7901 cells (Fig. 7A). The lower levels of growth were seen in KRT80 siRNA transfectants than the negative control by CCK-8 assay (Fig. 7B, $p<0.05$). There was a higher apoptosis in KRT80 siRNA transfectants than the negative control by Annexin V-PI double-staining (Fig. 7C, $p<0.05$). KRT80 knockdown inhibited migration and invasion as shown by wound healing (Fig. 7D, $p<0.05$) and transwell assay (Fig. 7E, $p<0.05$). KRT80 knockdown increased the expression of Bax, PARP-1, p38, p21, Beclin-1, Caspase-1, and E-cadherin, but decreased the expression of ki-67, p-Akt, p-stat3, Bcl-2, N-cadherin, Zeb1, slug, and MMP-9 in SGC-7901 cells (Fig. 7F).

Discussion

As an adaptive reaction to changes in gravity, extracellular matrix proteins, adhesion molecules, and cytoskeletal proteins build a dynamic network that interacts with signaling molecules. KRT80 is a filamentous protein, one of the major structural fibers that make up epithelial cells, and is significantly closer in structure to type II hair keratin than to type II

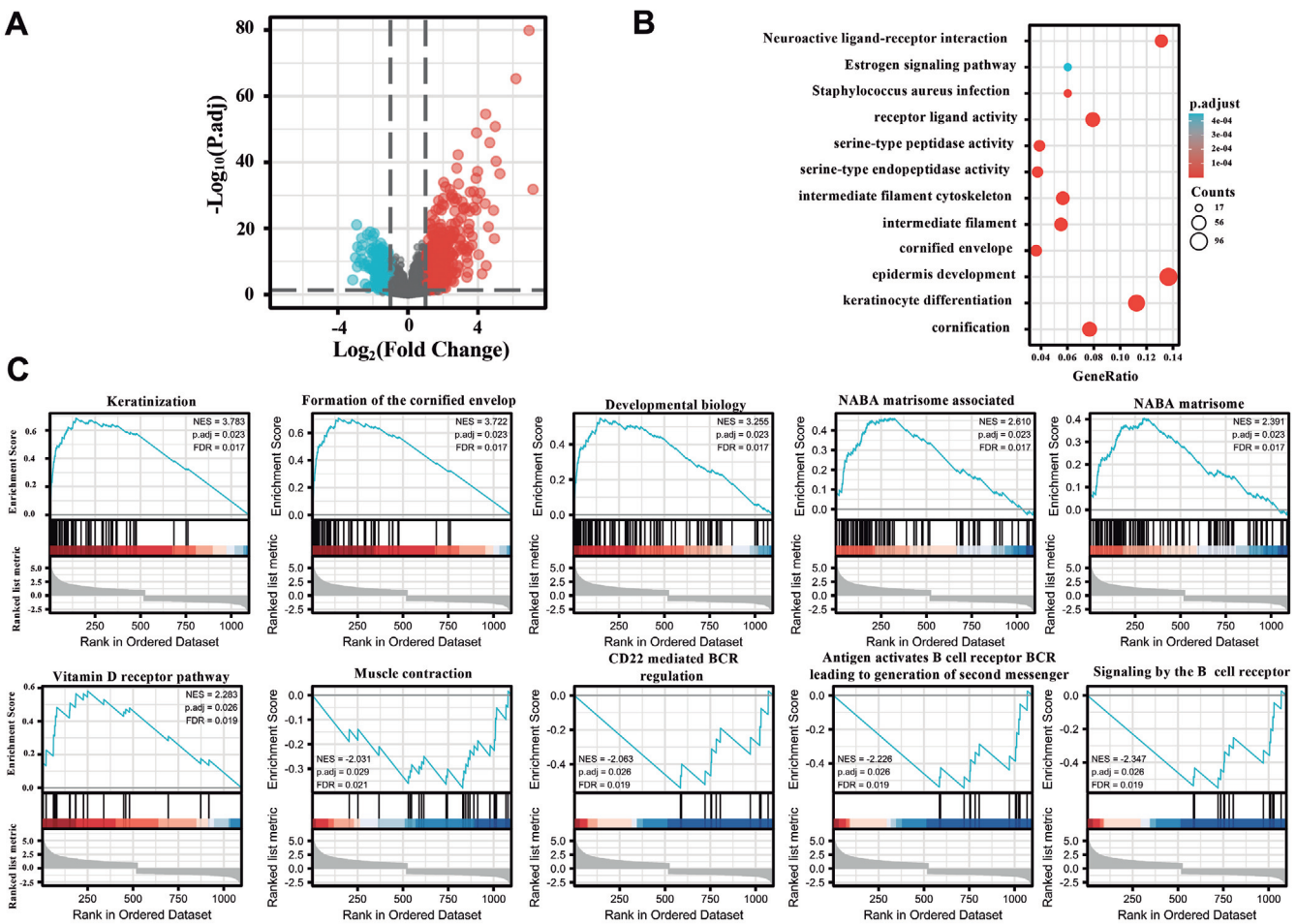

Fig. 3. The differential genes and related signal pathways of KRT80 expression in gastric cancer. A volcano map of the differential genes of KRT80 in gastric cancer **(A)**. These genes were subjected to signal pathway analysis using KEGG **(B)** and GSEA **(C)**.

epithelial keratin. Nonetheless, it is found in almost all types of epithelial cells, interacts with intermediate filament bundles close to the desmosomal plaques, and participates in cellular differentiation (Langbein et al., 2010). Although Castellucci et al. (2021). found that KRT80 mRNA expression was lower in cutaneous leishmaniasis than the control by GWAS, it was reported to up-regulate in colorectal cancer, lung cancer and gastric cancer according to the TCGA database or real-time RT-PCR (Lin et al., 2020; Ma et al., 2021; Tong et al., 2022; Zhang et al., 2022). Here, we noticed that KRT80 expression was higher in GC in combination of qRT-PCR, bioinformatics analysis, Western blot and immunohistochemistry. KRT80 expression was demonstrated to negatively correlate with the purity and loss of infiltration of immune cells in GC because it is a biomarker for epithelial cells. These data might illustrate the consistence in KRT80 expression between molecular and morphological detection, and indicated up-regulated KRT80 expression might be involved in gastric carcinogenesis. Here, we found a negative relationship between promoter methylation and the expression level of the KRT80 gene in GC, and KRT80 hypomethylation in GC, suggesting that KRT80 methylation might be

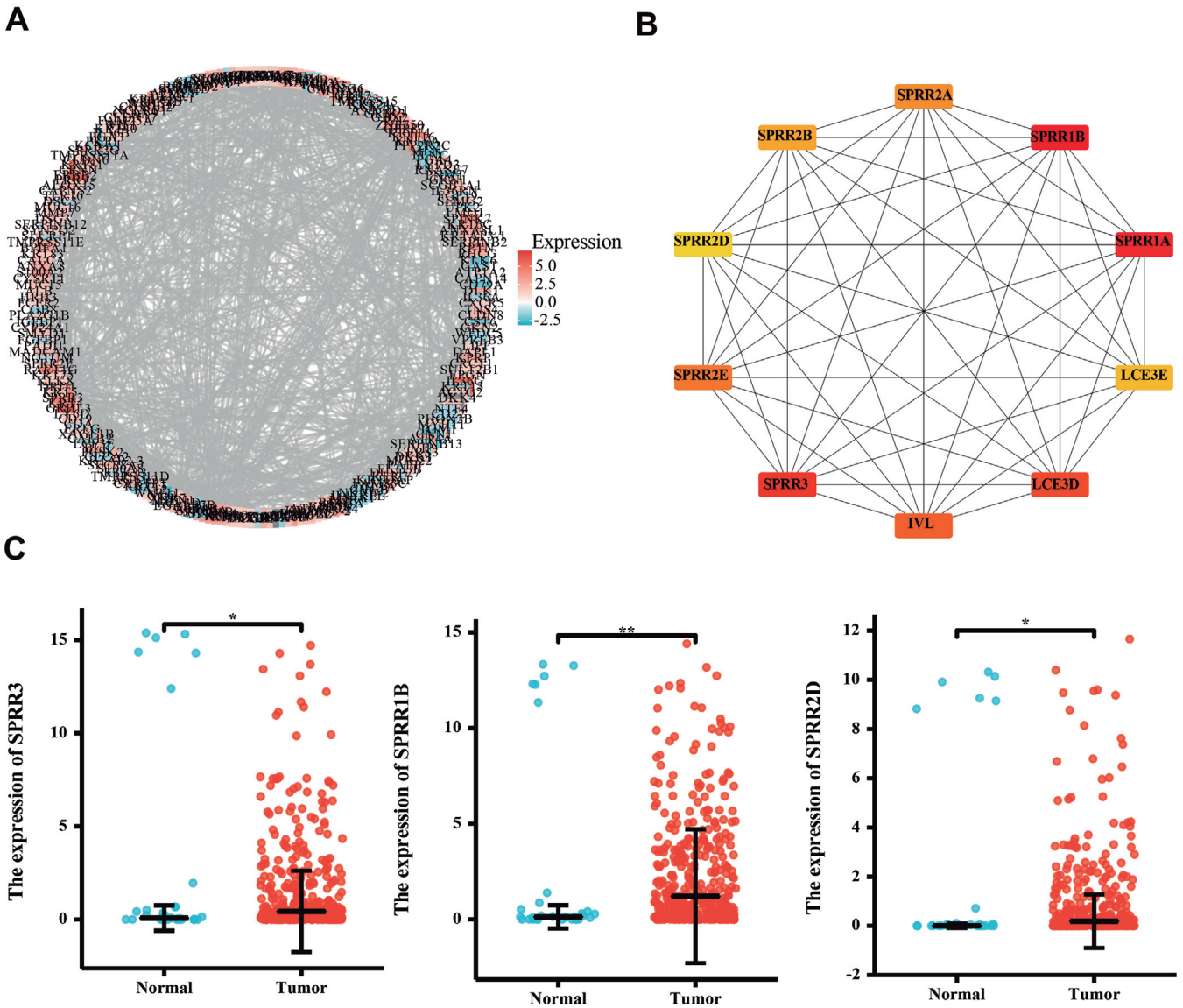

Fig. 4. PPI network and module analysis of differential genes of KRT80 in gastric cancer. STRING was used to identify the protein-protein interaction network of differential genes of KRT80 in gastric cancer **(A)**. Cytoscape was employed to find the top 10 hub nodes ranked by degree **(B)**. The hub genes were compared between gastric cancer and normal tissues **(C)**. *, $p<0.05$; **, $p<0.01$.

responsible for its down-regulation.

KRT80 expression was shown to be substantially related with increased lymph node and distant metastasis, as well as a higher pathological stage of colorectal cancer (Li et al., 2018; Ma et al., 2021), in agreement with the findings of GC (Zhang et al., 2022). In our study, KRT80 mRNA and protein expression were found to positively correlate with the differentiation of GC, which were the opposite for KRT80 methylation, indicating that KRT80 expression and methylation underlie the molecular foundation of gastric cancer differentiation and can be considered as a biomarker for the differentiation of GC. Moreover, KRT80 expression was significantly associated with lower disease-free survival, and overall survival in colorectal cancer patients as an independent prognostic indicator (Li et al., 2018). Sanada et al. (2019) found that KRT80 was a prognostic factor for lung adenocarcinoma patients by

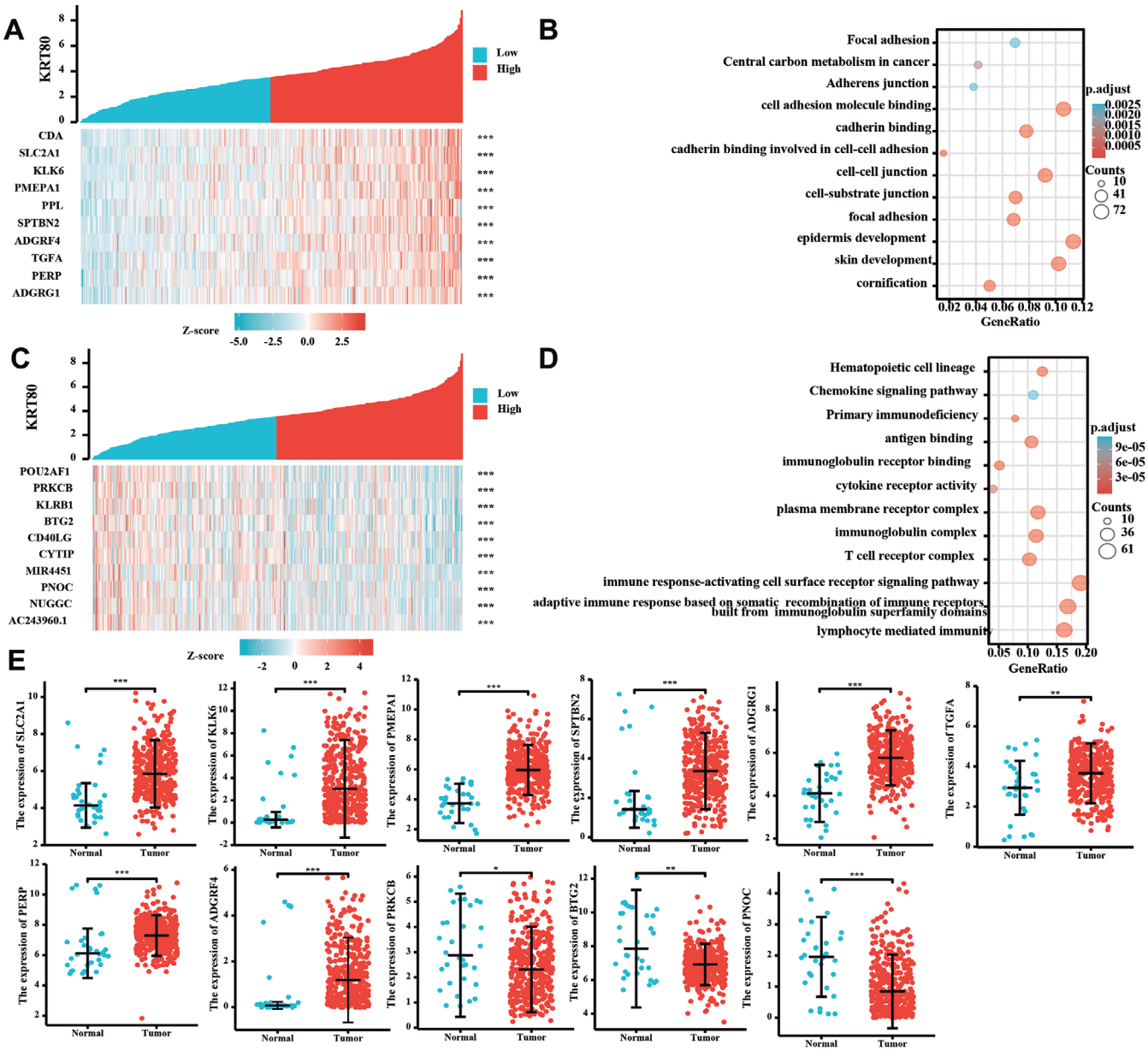

Fig. 5. The KRT80-related genes and signal pathways in gastric cancer. The top positively-related genes of KRT80 were screened according to the hot map **(A)**, and were classified into the signal pathway using xiantao database **(B)**. The top negatively-related genes of KRT80 were screened according to the hot map **(C)**, and were classified into the signal pathway using xiantao database **(D)**. The genes were compared between gastric cancer and normal tissue using xiantao platform **(E)**. *, p<0.05; **, p<0.01; ***, p<0.001.

Table 6. Relationship between KRT80 expression and clinicopathological features of gastric cancer according to immunohistochemistry.

Clinicopathological features	n	KRT80 expression				
		-	+	++	+++	PR(%)
Sex	261					
Male	197	58	63	59	17	70.6
Female	64	12	28	17	7	81.3
Age(years)						
<65	164	42	63	45	14	74.4
≥65	97	28	28	31	10	71.1
Depth of invasion						
Tis-1	30	9	8	11	2	70.0
T2-4	231	61	83	65	22	73.6
Lymphatic invasion						
–	139	43	41	40	15	69.1
+	110	25	45	33	7	77.3
Lymph node metastasis						
–	77	19	25	22	11	75.3
+	183	51	66	53	13	72.1
Distant metastasis						
–	251	67	88	74	22	73.3
+	10	3	3	2	2	70.0
Lauren's classification						
Intestinal-type	90	18	30	30	12	80.0
Mixed-type	29	6	6	15	2	79.3
Diffuse-type	132	43	52	29	8	67.4

PR, positive rate.

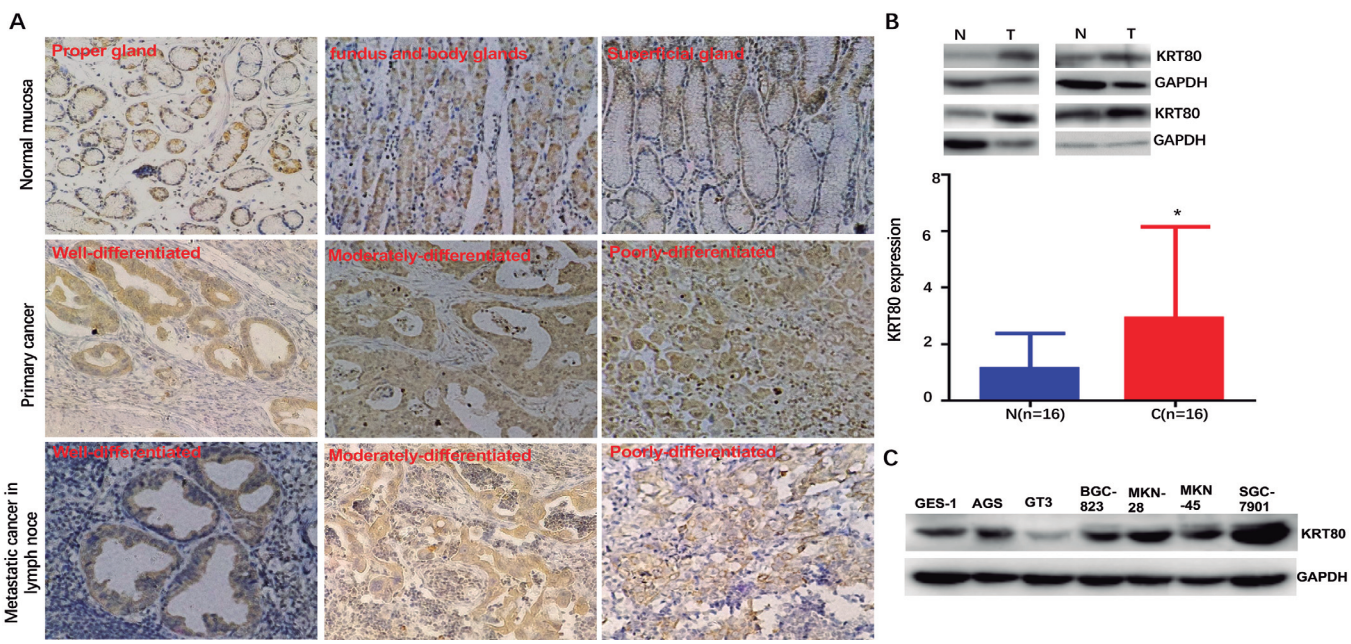

Fig. 6. The expression of KRT80 protein in gastric cancer. Immunohistochemically, KRT80 expression was positive in gastric superficial, fundus and body glands, but not in proper glands **(A)**. Western blot data showed a higher expression of KRT80 protein in gastric cancer than normal mucosa (**B**, $p<0.05$). KRT80 expression was screened in gastric epithelial and cancer cells by Western blot **(C)**. *, $p<0.05$

bioinformatics analysis of TCGA database. Here, we found that KRT80 mRNA expression was positively related to gastric cancer patients' short overall, progression-free, and post-progression survival times. Taken together, KRT80 mRNA expression might be employed as a risk factor for the prognosis of gastric cancer patients.

Furthermore, KRT80 expression promoted proliferation, migration, invasion and epithelial-mesenchymal transition (EMT) of colorectal cancer cells via the Akt pathway. KRT80 knockdown reduced the viability of colorectal cancer cells. KRT80 might interact with protein kinase, DNA-activated, catalytic polypeptide in colorectal cancer cells. KRT80-related genes were shown to be highly expressed in the cell cycle, DNA replication, immune system, protein and RNA metabolism, signal transduction, and other cellular processes (Li et al., 2018; Lin et al., 2020). CircPIP5K1A activated KRT80 to promote proliferation, invasion, migration and EMT of gastric cancer cells (Song et al., 2020), while TCONS_00049140 inactivated KRT80 to increase proliferation and melanin production of mouse melanocytes (Ji et al., 2018). Perone et al. (2019). demonstrated that SREBP1 drove KRT80-dependent cytoskeletal rearrangements and invasive behavior in endocrine-resistant and Erα-positive breast cancer. Rajagopalan et al. (2016). observed that KRT80 maintained epithelial barrier integrity in primary skin keratinocytes chronically exposed to cigarette smoke condensate. In the present study, the genes that are related to KRT80 were mostly involved in ligand-receptor interaction, peptidase, filament and cytoskeleton, keratinocyte differentiation, muscle contraction, and B cell-mediated immunity, cell adhesion and junction, and cadherin binding. KRT80 knockdown suppressed proliferation, anti-apoptosis, migration and invasion in gastric cancer cells in line with a previous report (Zhang et al., 2022) despite different kinds of cell lines used. These findings indicated that KRT80 might aggravate the aggressive phenotypes of gastric cancer cells by the above-mentioned pathways.

Both the PI3K/Akt and JAK-Stat3 pathways are frequently over-activated intracellular pathways and are involved in proliferation and anti-apoptosis in various cancers (Sanaei et al., 2022). P21 functions as a CDK inhibitor to arrest the cell cycle (He et al., 2022). Apoptosis is initiated when cell-surface death receptors like Fas are engaged by their ligands (the extrinsic pathway) or when pro-apoptotic Bcl-2-family proteins cause the permeabilization of the mitochondrial outer

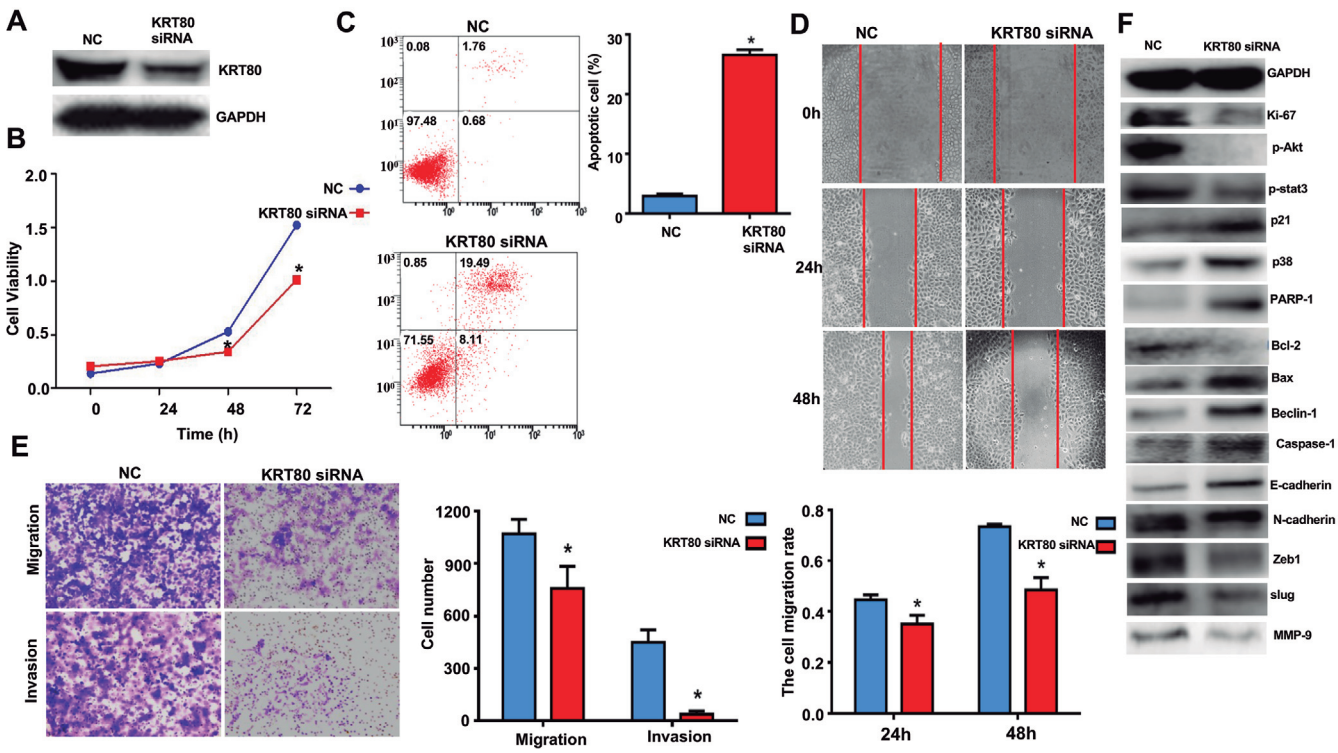

Fig. 7. The effects of KRT80 knockdown on the aggressive phenotypes and phenotype-related protein of gastric cancer cells. After siRNA transfection, KRT80 became weaker than SGC-7901 cells by Western blot **(A)**. The transfectants showed low growth **(B)**, high apoptosis **(C)**, low invasion and migration **(D, E)** in comparison to the parental cells. The phenotype-related proteins were screened by Western blot **(F)**. NC, negative control; *, $p<0.05$, compared with the negative control.

membrane (the intrinsic pathway), finally to activate Caspases (Lossi, 2022; Singh and Lim, 2022). When cellular stress activates MPAK p38 to mediate the interaction between Bax and Bcl-2 on the mitochondrial membrane, the opening of the mitochondrial voltage-dependent anion channel causes cytochrome c release and subsequent apoptosis. PARP1 may lead to apoptosis through caspase activation (He et al., 2022). By either inactivating Akt and stat3, decreasing Bcl-2/Bax, and increasing the expression of PARP1 and MAPK p38, KRT80 silencing inhibited proliferation and induced apoptosis in gastric cancer cells. Reportedly, pyroptosis is a recently discovered form of inflammatory programmed necrosis characterized by caspase-1 mediated cell death (Arakelian et al., 2022). Zeb1 and slug are found to promote the EMT with E-cadherin overexpression, and N-cadherin underexpression (Fedele et al., 2022). Therefore, we believed that KRT80 knockdown promoted the pyroptosis, and suppressed the EMT of GC by increasing Zeb1 and Slug.

In summary, up-regulated expression of KRT80 played an important role in gastric carcinogenesis, and might be considered as a biological marker for aggressive behaviors and poor prognosis. Its silencing might be used as a target therapy approach for gastric cancer patients.

Acknowledgements. Not applicable.

Funding. The present study was supported by Award for Liaoning Distinguished Professor, Emphasis Project of Education Department of Hebei Province (ZD2022096), Natural Science Foundation of Hebei Province (21377772D; H2022406034) and National Natural Science Foundation of China (81672700).

Availability of data and materials. The datasets used and/or analyzed are available from the corresponding author on reasonable request.

Authors' contributions. ZHC analyzed the data and contributed to the manuscript writing. SKH and XH performed the experiments. XLJ, ZEH and HZS helped to revise the draft.

Ethics approval and consent to participate. Yes

Patient consent for publication. Yes

Competing interests. The authors declare that they have no competing interests.

References

Arakelian T., Oosterhuis K., Tondini E., Los M., Vree J., van Geldorp M., Camps M., Teunisse B., Zoutendijk I., Arens R., Zondag G., Ossendorp F. and van Bergen J. (2022). Pyroptosis-inducing active caspase-1 as a genetic adjuvant in anti-cancer DNA vaccination. Vaccine 40, 2087-2098.

Bustin S. A., Benes V., Garson J. A., Hellemans J., Huggett J., Kubista M., Mueller R., Nolan T., Pfaffl M. W., Shipley G.L., Vandesompele J. and Wittwer C.T. (2009). The MIQE guidelines: minimum information for publication of quantitative real-time PCR experiments. Clin. Chem. 55, 611-622.

Castellucci L.C., Almeida L., Cherlin S., Fakiola M., Francis R.W., Carvalho E.M., Santos da Hora A., do Lago T.S., Figueiredo A.B., Cavalcanti C.M., Alves N.S., Morais K. L. P., Teixeira-Carvalho A., Dutra W.O., Gollob K.J., Cordell H.J. and Blackwell J.M. (2021). A genome-wide association study identifies SERPINB10, CRLF3, STX7, LAMP3, IFNG-AS1, and KRT80 as risk loci contributing to Cutaneous Leishmaniasis in Brazil. Clin. Infect. Dis. 72, e515-e525.

Fan X., Qin X., Zhang Y., Li Z., Zhou T., Zhang J., You W., Li W. and Pan K. (2021). Screening for gastric cancer in China: advances, challenges and visions. Chin. J. Cancer Res. 33, 168-180.

Fedele M., Sgarra R., Battista S., Cerchia L. and Manfioletti G. (2022). The epithelial-mesenchymal transition at the crossroads between metabolism and tumor progression. Int. J. Mol. Sci. 23, 800.

He S., Chakraborty R. and Ranganathan S. (2022). Proliferation and apoptosis pathways and factors in oral squamous cell carcinoma. Int. J. Mol. Sci. 23, 1562.

Ji K., Fan R., Zhang J., Yang S., and Dong C. (2018). Long non-coding RNA expression profile in Cdk5-knockdown mouse skin. Gene 672, 195-201.

Khajeh S., Tohidkia M. R., Aghanejad A., Mehdipour T., Fathi F. and Omidi Y. (2018). Phage display selection of fully human antibody fragments to inhibit growth-promoting effects of glycine-extended gastrin 17 on human colorectal cancer cells. Artif. Cells Nanomed. Biotechnol. 46 (Suppl. 2), 1082-1090.

Langbein L., Eckhart L., Rogers M.A., Praetzel-Wunder S. and Schweizer J. (2010). Against the rules: human keratin K80: two functional alternative splice variants, K80 and K80.1, with special cellular localization in a wide range of epithelia. J. Biol. Chem. 285, 36909-36921.

Li C., Liu X., Liu Y., Liu X., Wang R., Liao J., Wu S., Fan J., Peng Z., Li B. and Wang Z. (2018). Keratin 80 promotes migration and invasion of colorectal carcinoma by interacting with PRKDC via activating the AKT pathway. Cell Death Dis. 9, 1009.

Lin J., Fan X., Chen J., Xie X. and Yu H. (2020). Small interfering RNA-mediated knockdown of KRT80 suppresses colorectal cancer proliferation. Exp. Ther. Med. 20, 176.

Liu O., Wang C., Wang S., Hu Y., Gou R., Dong H., Li S., Li X. and Lin B. (2021). Keratin 80 regulated by miR-206/ETS1 promotes tumor progression via the MEK/ERK pathway in ovarian cancer. J. Cancer 12, 6835-6850.

Lossi L. (2022). The concept of intrinsic versus extrinsic apoptosis. Biochem. J. 479, 357-384.

Ma J., Wang P., Huang L., Qiao J., and Li J. (2021). Bioinformatic analysis reveals an exosomal miRNA-mRNA network in colorectal cancer. BMC Med. Genomics 14, 60.

Mehdipour T., Tohidkia M.R., Ata Saei A., Kazemi A., Khajeh S., Rahim Rahimi A.A., Nikfarjam S., Farhadi M., Halimi M., Soleimani R., Zubarev R.A. and Nouri M. (2020). Tailoring subtractive cell biopanning to identify diffuse gastric adenocarcinoma-associated antigens via human scFv antibodies. Immunology 159, 96-108.

Ouyang S., Zeng Z., Liu Z., Zhang Z., Sun J., Wang X., Ma M., Ye X., Yu J. and Kang W. (2022). OTUB2 regulates KRT80 stability via deubiquitination and promotes tumor proliferation in gastric cancer. Cell Death Dis. 8, 45.

Perone Y., Farrugia A.J., Rodríguez-Meira A., Győrffy B., Ion C., Uggetti A., Chronopoulos A., Marrazzo P., Faronato M., Shousha S., Davies C., Steel J.H., Patel N., Del Rio Hernandez A., Coombes C., Pruneri G., Lim A., Calvo F. and Magnani L. (2019). SREBP1 drives Keratin-80-dependent cytoskeletal changes and invasive behavior in endocrine-resistant ERα breast cancer. Nat. Commun. 10, 2115.

Rajagopalan P., Nanjappa V., Raja R., Jain A.P., Mangalaparthi K.K., Sathe G.J., Babu N., Patel K., Cavusoglu N., Soeur J., Pandey A.,

Roy N., Breton L., Chatterjee A., Misra N. and Gowda H. (2016). How does chronic cigarette smoke exposure affect human skin? a global proteomics study in primary human keratinocytes. OMICS 20, 615-626.

Sanada H., Seki N., Mizuno K., Misono S., Uchida A., Yamada Y., Moriya S., Kikkawa N., Machida K., Kumamoto T., Suetsugu T. and Inoue H. (2019). Involvement of dual strands of miR-143 (miR-143-5p and miR-143-3p) and their target oncogenes in the molecular pathogenesis of lung adenocarcinoma. Int. J. Mol. Sci. 20, 4482.

Sanaei M.J., Razi S., Pourbagheri-Sigaroodi A. and Bashash D. (2022). The PI3K/Akt/mTOR pathway in lung cancer; oncogenic alterations, therapeutic opportunities, challenges, and a glance at the application of nanoparticles. Transl. Oncol. 18, 101364.

Singh P. and Lim B. (2022). Targeting apoptosis in cancer. Curr. Oncol. Rep. 24, 273-284.

Song H., Xu Y., Xu T., Fan R., Jiang T., Cao M., Shi L. and Song J. (2020). CircPIP5K1A activates KRT80 and PI3K/AKT pathway to promote gastric cancer development through sponging miR-671-5p. Biomed. Pharmacother. 126, 109941.

Thrift A.P. and Nguyen T.H. (2021). Gastric cancer epidemiology. Gastrointest. Endosc. Clin. N. Am. 31, 425-439.

Tong Y., Chen X., Feng Z., Xu C. and Li Y. (2022). Keratin 80 promotes migration and invasion of non-small cell lung cancer cells by regulating the TGF-β/SMAD pathway. Evid. Based. Complement. Alternat. Med. 2022, 2630351.

Yang L., Ying X., Liu S., Lyu G., Xu Z., Zhang X., Li H., Li Q., Wang N. and Ji J. (2020). Gastric cancer: Epidemiology, risk factors and prevention strategies. Chin. J. Cancer Res. 32, 695-704.

Zhang F., Wang G., Yan W. and Jiang H. (2022). MiR-4268 suppresses gastric cancer genesis through inhibiting keratin 80. Cell Cycle 21, 2051-2064.

Accepted April 5, 2023